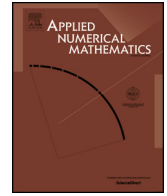




Contents lists available at [ScienceDirect](https://www.sciencedirect.com)

Applied Numerical Mathematics

www.elsevier.com/locate/apnum



A splitting uniformly convergent method for one-dimensional parabolic singularly perturbed convection-diffusion systems



C. Clavero ^{a,*}, J.C. Jorge ^b

^a Department of Applied Mathematics and IUMA, University of Zaragoza, Spain

^b Department of Computational and Mathematical Engineering and ISC, Public University of Navarra, Spain

ARTICLE INFO

Article history:

Received 29 July 2022

Received in revised form 22 September 2022

Accepted 22 September 2022

Available online 26 September 2022

Keywords:

Weakly coupled parabolic systems

Fractional Euler method

Splitting by components

Upwind scheme

Shishkin meshes

Uniform convergence

ABSTRACT

In this paper we deal with solving robustly and efficiently one-dimensional linear parabolic singularly perturbed systems of convection-diffusion type, where the diffusion parameters can be different at each equation and even they can have different orders of magnitude. The numerical algorithm combines the classical upwind finite difference scheme to discretize in space and the fractional implicit Euler method together with an appropriate splitting by components to discretize in time. We prove that if the spatial discretization is defined on an adequate piecewise uniform Shishkin mesh, the fully discrete scheme is uniformly convergent of first order in time and of almost first order in space. The technique used to discretize in time produces only tridiagonal linear systems to be solved at each time level; thus, from the computational cost point of view, the method we propose is more efficient than other numerical algorithms which have been used for these problems. Numerical results for several test problems are shown, which corroborate in practice both the uniform convergence and the efficiency of the algorithm.

© 2022 The Author(s). Published by Elsevier B.V. on behalf of IMACS. This is an open access article under the CC BY license (<http://creativecommons.org/licenses/by/4.0/>).

1. Introduction

In this work we consider an initial and boundary value problem for one-dimensional parabolic singularly perturbed coupled convection-diffusion systems. In the lowest dimensional case, there are two equations in the system and the considered problem can be written as follows.

Find $\mathbf{u}(x, t) : \overline{Q} \rightarrow \mathcal{R}^2$, a solution of

$$\begin{cases} \mathbf{L}_\epsilon \mathbf{u} \equiv \frac{\partial \mathbf{u}}{\partial t}(x, t) + \mathcal{L}_{x,\epsilon}(t)\mathbf{u}(x, t) = \mathbf{f}(x, t), & (x, t) \in Q, \\ \mathbf{u}(0, t) = \mathbf{g}_0(t), \mathbf{u}(1, t) = \mathbf{g}_1(t), t \in [0, T], \mathbf{u}(x, 0) = \boldsymbol{\varphi}(x), & x \in (0, 1), \end{cases} \quad (1)$$

where the spatial differential operator $\mathcal{L}_{x,\epsilon}(t)$ is defined as

$$\mathcal{L}_{x,\epsilon}(t)\mathbf{u} \equiv -\mathcal{D}_\epsilon \frac{\partial^2 \mathbf{u}}{\partial x^2} + \mathcal{B}(x) \frac{\partial \mathbf{u}}{\partial x} + \mathcal{A}(x, t)\mathbf{u}, \quad (2)$$

* Corresponding author.

E-mail addresses: clavero@unizar.es (C. Clavero), [jcyjorge@unavarra.es](mailto:jcjorge@unavarra.es) (J.C. Jorge).

$Q \equiv \Omega \times (0, T]$ with $\Omega = (0, 1)$, $\mathbf{u} = (u_1, u_2)^T$, the diffusion matrix is $\mathcal{D}_\varepsilon = \text{diag}(\varepsilon_1, \varepsilon_2)$, the convection matrix is $\mathcal{B}(x) = \text{diag}(b_{11}(x), b_{22}(x))$, the reaction matrix is $\mathcal{A}(x, t) = (a_{kp}(x, t))$, $k, p = 1, 2$, $\mathbf{g}_0 = (g_{1,0}, g_{2,0})^T$, $\mathbf{g}_1 = (g_{1,1}, g_{2,1})^T$, and $\boldsymbol{\varphi} = (\varphi_1, \varphi_2)^T$.

Henceforth, we suppose that the equations of (1) have been ordered and scaled in such a way that $0 < \varepsilon_1 \leq \varepsilon_2 \leq 1$; also, we assume that the diffusion parameters ε_k , $k = 1, 2$ can be very small and, besides, they can have different order of magnitude. Let $\boldsymbol{\varepsilon} = (\varepsilon_1, \varepsilon_2)^T$. Moreover, the coefficients of the convection matrix satisfy

$$b_{kk}(x) \geq \beta > 0, \quad k = 1, 2, \tag{3}$$

and the coefficients of the reaction matrix \mathcal{A} satisfy

$$a_{kk} \geq 0, \quad a_{kp} \leq 0, \quad \text{if } k \neq p \text{ and } \sum_{p=1}^2 a_{kp} \geq 0, \quad k, p \in \{1, 2\}, \quad \forall (x, t) \in \overline{Q}. \tag{4}$$

Notice that we have weakened somewhat the usual restrictions imposed for the reaction matrix in many works for singularly perturbed coupled systems (see [2,6,12,20,24]); here, \mathcal{A} is not necessarily an M -matrix.

Problems of this type have been considered in several recent papers; for instance, in [13] a two-dimensional version of (1) is considered and it is proved that this problem has a unique solution. In [13], the authors follow the ideas developed in [11] for proving the existence and uniqueness of a solution to a stationary coupled system. Such techniques can also be used in our problem to deduce the existence and uniqueness of a solution. Moreover, in [20] it is shown that the solution of (1) has overlapping boundary layers of width $\mathcal{O}(\varepsilon_k |\ln \varepsilon_k|)$, $k = 1, 2$ at the outflow boundary $x = 1$. Therefore, uniformly convergent methods are needed to find good numerical approximations for arbitrary values of the diffusion parameters with a reasonable computational cost. To assure that the exact solution $\mathbf{u} \in C^{4,2}(\overline{Q})$, we assume that the source term of the differential equation, $\mathbf{f}(x, t) = (f_1, f_2)^T$, the initial and boundary conditions as well as the coefficients of the differential equations are sufficiently smooth functions, and that sufficient compatibility conditions among all of these data hold (see [16] for a detailed discussion).

Singularly perturbed convection-diffusion coupled systems model many physical phenomena like, for instance, diffusion-convection enzyme models, tubular models in chemical reactor theory or neutron transport problems with diffusion coefficients (see [23]); because of that, these problems and the construction and analysis of efficient numerical schemes to solve them have received much attention in the recent years. In [1,17,19,24], 1D convection-diffusion elliptic systems with equal or different diffusion parameters at each equation of the system were analyzed. In [20], problem (1) was also considered and in [14] a similar problem to (1) but with discontinuous coefficients in the convection matrix was considered. In [25] another case with an additional coupling in the convective terms but with equal diffusion parameters was analyzed. In [18] an elliptic 2D system of convection-diffusion type was considered. In all of these cases, the computational cost of the methods is, in general, substantially increased, in comparison with analogue schemes for singularly perturbed scalar convection diffusion equations, due to the coupling of the components of the discrete solution. To reduce this computational cost, an iterative scheme was proposed in [22] for a stationary reaction-diffusion system, the Schwarz domain decomposition method was used in [27] and in [3,4], additive schemes were analyzed for 1D and 2D parabolic reaction-diffusion systems respectively. The additive schemes reduce the computational cost, because they decouple the components of the discrete solution in such a way that only tridiagonal or block tridiagonal, respectively, linear systems must be solved at each time level of the discretization. Nevertheless, the analysis of the uniform convergence is quite tricky.

With a similar aim of computational cost reduction, the splitting by components technique was proposed in [6] to solve a 1D parabolic system of reaction-diffusion type with an arbitrary number of equations; the same idea was applied in [7] to solve efficiently a coupled 2D parabolic system of convection-diffusion type which has the same diffusion parameter in all equations of the system. In this paper we adapt this technique to solve efficiently problem (1). This technique permits also to calculate the numerical approximation of the solution decoupling the components of the system. The numerical algorithm is easy to implement and the analysis of its uniform convergence is considerably simpler than the one developed for the additive schemes. Moreover, the ideas exposed in this paper can be extended to coupled systems with an arbitrary number of equations.

The paper is structured as follows. In section 2, we study the asymptotic behavior of the exact solution of the continuous problem and we obtain appropriate estimates for its derivatives which describe the asymptotic behavior of the solution with respect to the diffusion parameters. In Section 3, we construct a spatial semidiscretization of the continuous problem; for that, we use the upwind scheme defined on a nonuniform mesh of Shishkin type obtaining a family of stiff Initial Value Problems and we prove that their solutions converge uniformly to the solution of (1) with the order of almost one. In section 4, we give our proposal for an efficient time integration of the stiff Initial Value Problems derived from the previous semidiscretization stage. This process combines the fractional implicit Euler method joint to a splitting by components (see [5]) and we prove that it is a first order uniformly convergent method. In Section 5, the numerical results for some test problems are shown; from them we can observe the uniformly convergent behavior of the algorithm and also its efficiency in comparison with other classical methods. We also include the results for a coupled system with a higher number of equations, showing that our technique can be successfully applied to systems with an arbitrary number of equations. Finally, in Section 6, some conclusions are given.

Henceforth, C denotes a generic positive constant independent of the diffusion parameters ε_k , $k = 1, 2$ and the discretization parameters N and M , and $\mathbf{C} = (C, C)^T$. Also $\mathbf{v} \leq \mathbf{w}$ means that $v_k \leq w_k$, $k = 1, 2$, $|\mathbf{v}| = (|v_1|, |v_2|)^T$ and $\|\mathbf{f}\|_G = \max\{\|f_1\|_G, \|f_2\|_G\}$ where $\|f\|_G$ is the maximum norm of f on the closed set G .

2. Asymptotic behavior of the exact solution

In this section we study the asymptotic behavior of the solution \mathbf{u} of (1) and we obtain appropriate estimates for its derivatives; from them, we deduce the existence of overlapping boundary layers on $x = 1$. Such estimates arise from the following inverse positivity result, and its subsequent uniform bounding for the solution of (1); the proof is similar to the ones in [2] for the elliptic case and in [12] for the parabolic case.

Lemma 1 (Maximum principle). *Let $\mathbf{w} \in C(\bar{Q}) \cap C^2(Q)$ be such that $\mathcal{L}_\varepsilon(t)\mathbf{w} \geq \mathbf{0}$ on Q , such that $\mathbf{w} \geq \mathbf{0}$ on $\{0, 1\} \times [0, T]$. Then, $\mathbf{w} \geq \mathbf{0}$, $\forall(x, t) \in \bar{Q}$.*

Notice that the previous lemma guarantees the uniqueness of the solution of (1).

Lemma 2 (Uniform bounding). *The exact solution of (1) satisfies*

$$\|\mathbf{u}\|_{\bar{Q}} \leq \max\{\|\boldsymbol{\varphi}\|_{[0,1]}, \|\mathbf{g}_0\|_{[0,T]}, \|\mathbf{g}_1\|_{[0,T]}\} + \frac{1}{\beta} \|\mathbf{f}\|_{\bar{Q}} \tag{5}$$

Following the ideas in [9], using Lemma 1 and appropriate barrier functions it is not difficult to prove that the exact solution of (1) satisfies

$$\left| \frac{\partial^r u_k}{\partial t^r} \right| \leq C, \quad r = 0, 1, 2, \quad k = 1, 2. \tag{6}$$

Lemma 3. *The components u_k , $k = 1, 2$ of \mathbf{u} solution of (1) satisfy*

$$\begin{aligned} \left| \frac{\partial^l u_k}{\partial x^l} \right| &\leq C\varepsilon_k^{-l}, \quad l = 1, 2, \quad k = 1, 2, \\ \left| \frac{\partial^3 u_1}{\partial x^3} \right| &\leq C\varepsilon_1^{-1}(\varepsilon_1^{-2} + \varepsilon_2^{-1}), \quad \left| \frac{\partial^3 u_2}{\partial x^3} \right| \leq C\varepsilon_2^{-1}(\varepsilon_1^{-1} + \varepsilon_2^{-2}). \end{aligned} \tag{7}$$

Proof. It is an easy adaptation of Lemma 3 in [2]. \square

The estimates (7) are not sufficiently fine globally and do not reflect in detail the boundary layer behavior of \mathbf{u} near $x = 1$; therefore, they are not adequate to analyze the uniform convergence of the spatial discretization in next section. To refine those estimates, we decompose the exact solution as $\mathbf{u} = \mathbf{v} + \mathbf{w}$ where \mathbf{v} is called the regular component and \mathbf{w} is the singular component. The regular component \mathbf{v} is the solution of the problem

$$\begin{cases} L_\varepsilon \mathbf{v} = \mathbf{f}, & \text{in } Q, \\ \mathbf{v}(x, 0) = \boldsymbol{\varphi}(x), & x \in [0, 1], \\ \mathbf{v}(0, t) = \mathbf{g}(0, t), & t \in [0, T], \\ \mathbf{v}(1, t) = \mathbf{v}_1(t), & t \in [0, T], \end{cases} \tag{8}$$

and the singular component \mathbf{w} is the solution of the problem

$$\begin{cases} L_\varepsilon \mathbf{w} = \mathbf{0}, & \text{in } Q, \\ \mathbf{w}(x, 0) = \mathbf{u}(x, 0) - \mathbf{v}(x, 0), & x \in [0, 1], \\ \mathbf{w}(0, t) = \mathbf{u}(0, t) - \mathbf{v}(0, t), & t \in [0, T], \\ \mathbf{w}(1, t) = \mathbf{u}(1, t) - \mathbf{v}_1(t), & t \in [0, T], \end{cases} \tag{9}$$

where $\mathbf{v}_1(t)$ is chosen appropriately.

Lemma 4. *The regular component $\mathbf{v} = (v_1, v_2)^T$ satisfies*

$$\begin{aligned} \left| \frac{\partial^r v_k}{\partial t^r} \right| &\leq C, \quad r = 0, 1, 2, \quad \left| \frac{\partial^l v_k}{\partial x^l} \right| \leq C, \quad l = 1, 2, \quad \left| \frac{\partial^2 v_k}{\partial t \partial x} \right| \leq C, \quad \left| \frac{\partial^3 v_k}{\partial t \partial x^2} \right| \leq C, \quad k = 1, 2, \\ \left| \frac{\partial^3 v_1}{\partial x^3} \right| &\leq C\varepsilon_1^{-1}, \quad \left| \frac{\partial^3 v_2}{\partial x^3} \right| \leq C\varepsilon_2^{-1}. \end{aligned} \tag{10}$$

Proof. The proof follows the usual ideas in the context of singularly perturbed problems and it adapts the ideas in [10], where a weakly coupled system of convection-diffusion type in the stationary case was considered. First, we write the components of \mathbf{v} in the form

$$v_k = v_{k,0} + \varepsilon_2 v_{k,1} + \varepsilon_2^2 v_{k,2}, \quad k = 1, 2, \tag{11}$$

where $v_{k,p}$, $k = 1, 2$, $p = 0, 1, 2$ are the solution of the following problems:

$$\begin{aligned} \frac{\partial v_{1,0}}{\partial t} + b_1 \frac{\partial v_{1,0}}{\partial x} + a_{11} v_{1,0} + a_{12} v_{2,0} &= f_1, \quad v_{1,0}(0, t) = g_{1,0}(t), \quad v_{1,0}(x, 0) = \varphi_1(x), \\ \frac{\partial v_{2,0}}{\partial t} + b_2 \frac{\partial v_{2,0}}{\partial x} + a_{21} v_{1,0} + a_{22} v_{2,0} &= f_2, \quad v_{2,0}(0, t) = g_{2,0}(t), \quad v_{2,0}(x, 0) = \varphi_2(x), \\ \frac{\partial v_{1,1}}{\partial t} + b_1 \frac{\partial v_{1,1}}{\partial x} + a_{11} v_{1,1} + a_{12} v_{2,1} &= \frac{\varepsilon_1}{\varepsilon_2} \frac{\partial^2 v_{1,0}}{\partial x^2}, \quad v_{1,1}(0, t) = 0, \quad v_{1,1}(x, 0) = 0, \\ \frac{\partial v_{2,1}}{\partial t} + b_2 \frac{\partial v_{2,1}}{\partial x} + a_{21} v_{1,1} + a_{22} v_{2,1} &= \frac{\partial^2 v_{2,0}}{\partial x^2}, \quad v_{2,1}(0, t) = 0, \quad v_{2,1}(x, 0) = 0, \\ \frac{\partial v_{1,2}}{\partial t} - \varepsilon_1 \frac{\partial^2 v_{1,2}}{\partial x^2} + b_1 \frac{\partial v_{1,2}}{\partial x} + a_{11} v_{1,2} + a_{12} v_{2,2} &= \frac{\varepsilon_1}{\varepsilon_2} \frac{\partial^2 v_{1,1}}{\partial x^2}, \\ v_{1,2}(0, t) = 0, \quad v_{1,2}(1, t) = 0, \quad v_{1,2}(x, 0) = 0, \\ \frac{\partial v_{2,2}}{\partial t} - \varepsilon_2 \frac{\partial^2 v_{2,2}}{\partial x^2} + b_2 \frac{\partial v_{2,2}}{\partial x} + a_{21} v_{1,2} + a_{22} v_{2,2} &= \frac{\partial^2 v_{2,1}}{\partial x^2}, \\ v_{2,2}(0, t) = 0, \quad v_{2,2}(1, t) = 0, \quad v_{2,2}(x, 0) = 0. \end{aligned} \tag{12}$$

Then, trivially it holds

$$\frac{\partial^{r+l} v_{k,p}}{\partial t^r \partial x^l} \leq C, \quad k = 1, 2, \quad p = 0, 1, \quad 0 \leq r + l \leq 3. \tag{13}$$

Moreover, using Lemma 3 it follows

$$\frac{\partial^l v_{2,2}}{\partial x^l} \leq C \varepsilon_2^{-l}, \quad l = 0, 1, 2. \tag{14}$$

To obtain more precise estimates, we now decompose $v_{1,2}$ in the form

$$v_{1,2} = q_0 + \varepsilon_1 q_1 + \varepsilon_1^2 q_2 \tag{15}$$

where

$$\begin{aligned} \frac{\partial q_0}{\partial t} + b_1 \frac{\partial q_0}{\partial x} + a_{11} q_0 + a_{12} v_{2,2} &= \frac{\varepsilon_1}{\varepsilon_2} \frac{\partial^2 v_{1,1}}{\partial x^2}, \quad q_0(0, t) = 0, \quad q_0(x, 0) = 0, \\ \frac{\partial q_1}{\partial t} + b_1 \frac{\partial q_1}{\partial x} + a_{11} q_1 &= \frac{\partial^2 q_0}{\partial x^2}, \quad q_1(0, t) = 0, \quad q_1(x, 0) = 0, \\ \frac{\partial q_2}{\partial t} - \varepsilon_1 \frac{\partial^2 q_2}{\partial x^2} + b_1 \frac{\partial q_2}{\partial x} + a_{11} q_2 &= \frac{\partial^2 q_1}{\partial x^2}, \\ q_2(0, t) = 0, \quad q_2(1, t) = 0, \quad q_2(x, 0) = 0. \end{aligned}$$

Then, following to [22] we can obtain

$$\frac{\partial^l v_{1,2}}{\partial x^l} \leq C \varepsilon_2^{-l}, \quad l = 1, 2, \quad \frac{\partial^3 v_{1,2}}{\partial x^3} \leq C \varepsilon_1^{-1} \varepsilon_2^{-2}. \tag{16}$$

Finally, differentiating respect to x the last equation in (12), from (13)-(16) we deduce

$$\frac{\partial^3 v_{2,2}}{\partial x^3} \leq C \varepsilon_2^{-3}. \tag{17}$$

Taking into account the decompositions (11) and (15), the required result follows. \square

Remark 1. Note that $\mathbf{v}_1(t)$ is given by adding the values at $x = 1$ of the functions which appear in (11) and (15).

Next, we study the singular component; to simplify the presentation we denote

$$B_\gamma(x) = e^{-\beta(1-x)/\gamma}, \tag{18}$$

where γ is any positive constant and β is defined in (3).

Lemma 5. The singular component $\mathbf{w} = (w_1, w_2)^T$ satisfies

$$\left| \frac{\partial^r w_k}{\partial t^r} \right| \leq C B_{\varepsilon_2}(x), \quad r = 0, 1, 2, \quad k = 1, 2, \tag{19}$$

$$\left| \frac{\partial^l w_1}{\partial x^l} \right| \leq C \left(\varepsilon_1^{-l} B_{\varepsilon_1}(x) + \varepsilon_2^{-l+1} B_{\varepsilon_2}(x) \right), \quad l = 1, 2, 3, \tag{20}$$

$$\left| \frac{\partial^l w_2}{\partial x^l} \right| \leq C \varepsilon_2^{-l} B_{\varepsilon_2}(x), \quad l = 1, 2, \tag{21}$$

$$\left| \frac{\partial^3 w_2}{\partial x^3} \right| \leq C \varepsilon_2^{-1} \left(\varepsilon_1^{-1} B_{\varepsilon_1}(x) + \varepsilon_2^{-2} B_{\varepsilon_2}(x) \right). \tag{22}$$

Proof. Taking into account (6), proceeding as in [2], we define the barrier function $\psi = (CB_{\varepsilon_2}(x), CB_{\varepsilon_2}(x))^T$. Then, trivially it holds $\mathcal{L}_\varepsilon(t)\mathbf{w} \geq \mathbf{0}$ and from Lemma 1, the estimate (19) for $r = 0$ follows.

Moreover, the technique developed in [9], together with Lemma 1 and the same barrier function ψ permits to prove that

$$\left| \frac{\partial^r w_k}{\partial t^r} \right| \leq C B_{\varepsilon_2}(x), \quad r = 1, 2, \quad k = 1, 2. \tag{23}$$

From problem (9), if we denote $z_{1,1} = \frac{\partial w_1}{\partial x}$ we have

$$-\varepsilon_1 \frac{\partial z_{1,1}}{\partial x} + b_1 z_{1,1} = -(a_{11} w_1 + a_{12} w_2) - \frac{\partial w_1}{\partial t} \equiv h_{1,1}(x, t),$$

with $|h_{1,1}(x, t)| \leq C B_{\varepsilon_2}(x)$. Then, the technique in [15] proves that it holds

$$\left| \frac{\partial w_1}{\partial x} \right| \leq C \varepsilon_1^{-1} B_{\varepsilon_1}(x). \tag{24}$$

In the same way, using the second equation in (9) we can obtain

$$\left| \frac{\partial w_2}{\partial x} \right| \leq C \varepsilon_2^{-1} B_{\varepsilon_2}(x). \tag{25}$$

Now, differentiating once with respect to x the first equation in (9) and denoting $z_{1,2} = \frac{\partial^2 w_1}{\partial x^2}$, we have

$$-\varepsilon_1 \frac{\partial z_{1,2}}{\partial x} + b_1 z_{1,2} = -\frac{\partial(a_{11} w_1 + a_{12} w_2)}{\partial x} - \frac{\partial^2 w_1}{\partial t \partial x} - \frac{\partial b_1}{\partial x} \frac{\partial w_1}{\partial x} \equiv h_{1,2}(x, t).$$

Following to [9] we can deduce $|h_{1,2}(x, t)| \leq C \left(\varepsilon_1^{-1} B_{\varepsilon_1}(x) + \varepsilon_2^{-1} B_{\varepsilon_2}(x) \right)$, and therefore the technique in [15] permits to prove

$$\left| \frac{\partial^2 w_1}{\partial x^2} \right| \leq C \left(\varepsilon_1^{-2} B_{\varepsilon_1}(x) + \varepsilon_2^{-1} B_{\varepsilon_2}(x) \right). \tag{26}$$

Differentiating respect to x the second equation in (9), similarly we can deduce

$$\left| \frac{\partial^2 w_2}{\partial x^2} \right| \leq C \varepsilon_2^{-2} B_{\varepsilon_2}(x). \tag{27}$$

Differentiating twice with respect to x the first equation in (9) and repeating the previous procedure we can obtain

$$\left| \frac{\partial^3 w_1}{\partial x^3} \right| \leq C \left(\varepsilon_1^{-3} B_{\varepsilon_1}(x) + \varepsilon_2^{-2} B_{\varepsilon_2}(x) \right). \tag{28}$$

Finally, differentiating once with respect to x the second equation in (9) we have

$$-\varepsilon_2 \frac{\partial^3 w_2}{\partial x^3} + b_2 \frac{\partial^2 w_2}{\partial x^2} = -\frac{\partial(a_{21} w_1 + a_{22} w_2)}{\partial x} - \frac{\partial^2 w_2}{\partial t \partial x} - \frac{\partial b_2}{\partial x} \frac{\partial w_2}{\partial x} \equiv h_{1,2}(x, t),$$

and using the previous estimates, directly it follows

$$\left| \frac{\partial^3 w_2}{\partial x^3} \right| \leq C \varepsilon_2^{-1} \left(\varepsilon_1^{-1} B_{\varepsilon_1}(x) + \varepsilon_2^{-2} B_{\varepsilon_2}(x) \right). \tag{29}$$

From (24)-(29) the required result follows. \square

Remark 2. Following the ideas of [2,10], where a weakly coupled convection-diffusion system in the stationary case was considered, we could obtain the estimates

$$\left| \frac{\partial^l w_1}{\partial x^l} \right| \leq C \left(\varepsilon_1^{-l} B_{\varepsilon_1}(x) + \varepsilon_2^{-l} B_{\varepsilon_2}(x) \right), \quad l = 1, 2, 3,$$

for the derivatives of the first component w_1 of the singular component, which suggests a stronger influence of the solution of the second equation in the system into the first one, which is not so precise as the estimates in Lemma 5 provide. Moreover, the estimates (19) for the derivatives of the second component are better than those ones given in [12,20].

3. The spatial discretization on a Shishkin mesh

To discretize problem (1) in space, we use the simple upwind scheme. From the knowledge of the behavior of the exact solution which we have described in the previous section, we are ready to choose a suitable mesh, capable of capturing its boundary layer behavior at $x = 1$. For that, we construct an adequate piecewise uniform mesh of Shishkin type, $\bar{\Omega}^N \equiv \{0 = x_0 < x_1 < \dots < x_N = 1\}$, which is defined as follows (see [18]). Let N be a positive integer divisible by 3; we define the transition parameters

$$\sigma_{\varepsilon_2} = \min \{2/3, \sigma_0 \varepsilon_2 \ln N\}, \quad \sigma_{\varepsilon_1} = \min \{\sigma_{\varepsilon_2}/2, \sigma_0 \varepsilon_1 \ln N\}, \tag{30}$$

which separate the coarse and the fine mesh, where σ_0 is a constant to be fixed later such that

$$\sigma_0 \geq \frac{2}{\beta}. \tag{31}$$

Then, the grid points are given by

$$x_i = \begin{cases} iH, & i = 0, \dots, N/3, \\ x_{N/3} + (i - N/3)h_{\varepsilon_2}, & i = N/3 + 1, \dots, 2N/3, \\ x_{2N/3} + (i - 2N/3)h_{\varepsilon_1}, & i = 2N/3 + 1, \dots, N, \end{cases} \tag{32}$$

with $H = 3(1 - \sigma_{\varepsilon_2})/N$, $h_{\varepsilon_2} = 3(\sigma_{\varepsilon_2} - \sigma_{\varepsilon_1})/N$, $h_{\varepsilon_1} = 3\sigma_{\varepsilon_1}/N$. We denote by $h_i = x_i - x_{i-1}$, $i = 1, \dots, N$, and $\bar{h}_i = (h_i + h_{i+1})/2$, $i = 1, \dots, N - 1$.

Let us denote by Ω^N the subgrid of $\bar{\Omega}^N$ composed only by the interior points of it, i.e., by $\bar{\Omega}^N \cap \Omega$, by $[\mathbf{v}]_{\Omega^N}$ (analogously $[v]_{\Omega^N}$ for scalar functions) the restriction operators, applied to vector functions defined on Ω , to the mesh Ω^N . For all $x_i \in \Omega^N$, we introduce the semidiscretization approach $\mathbf{U}^N(t) \equiv (\mathbf{U}_i^N(t))$, $i = 1, \dots, N - 1$, with $\mathbf{U}_i^N(t) \equiv (U_{1,i}, U_{2,i})^T \approx \mathbf{u}(x_i, t)$, as the solution of the following Initial Value Problem

$$\begin{cases} \mathbf{L}_{\varepsilon}^N \mathbf{U}^N \equiv \frac{d\mathbf{U}^N}{dt}(t) + \mathcal{L}_{\varepsilon}^N(t) \bar{\mathbf{U}}^N(t) = [\mathbf{f}(x, t)]_{\Omega^N}, & \text{in } \Omega^N \times [0, T], \\ \mathbf{U}_0^N(t) = \mathbf{g}_0(t), & \text{in } [0, T], \\ \mathbf{U}_1^N(t) = \mathbf{g}_1(t), & \text{in } [0, T], \\ \mathbf{U}^N(0) = [\varphi(x)]_{\Omega^N}, \end{cases} \tag{33}$$

where $\bar{\mathbf{U}}^N(t)$ is the natural extension to $\bar{\Omega}^N \times [0, T]$ of the semidiscrete functions $\mathbf{U}^N(t)$, defined on $\Omega^N \times [0, T]$, by adding the corresponding boundary data. Here $\mathcal{L}_{\varepsilon}^N(t)$ is the discretization of the operator $\mathcal{L}_{x,\varepsilon}(t)$ using the upwind scheme. i.e., for any sufficiently smooth continuous function $z(x, t)$ we use the approximations

$$\delta_x^2 z(x_i, t) = \frac{1}{\bar{h}_i} \left(\frac{z(x_{i+1}, t) - z(x_i, t)}{h_{i+1}} - \frac{z(x_i, t) - z(x_{i-1}, t)}{h_i} \right)$$

for the second derivative and

$$D_x^- z(x_i, t) = \frac{z(x_i, t) - z(x_{i-1}, t)}{h_i}$$

for the first derivative respectively, at the grid point x_i . Then, the numerical scheme can be written as

$$(\mathcal{L}_{\varepsilon}^N(t) \bar{\mathbf{U}}^N)_{k,i} = r_{k,i}^- \bar{U}_{k,i-1}^N + r_{k,i}^+ \bar{U}_{k,i+1}^N + r_{k,i}^c \bar{U}_{k,i}^N + a_{k1}(x_i, t) \bar{U}_{1,i}^N + a_{k2}(x_i, t) \bar{U}_{2,i}^N, \tag{34}$$

with

$$r_{k,i}^- = \frac{-\varepsilon_k}{h_i \bar{h}_i} - \frac{b_{kk}(x_i)}{h_i}, \quad r_{k,i}^+ = \frac{-\varepsilon_k}{h_{i+1} \bar{h}_i}, \quad r_{k,i}^c = -(r_{k,i}^- + r_{k,i}^+), \tag{35}$$

for $k = 1, 2$ and $i = 1, \dots, N - 1$. Below we denote $\mathcal{L}_{\varepsilon}^N(t) = (\mathcal{L}_{\varepsilon,1}^N(t), \mathcal{L}_{\varepsilon,2}^N(t))^T$.

The uniform well-posedness of (33) is a consequence of the following semidiscrete maximum principle (see [7]).

Lemma 6. Under the assumption $[\mathbf{f}(x, t)]_{\Omega^N} \leq \mathbf{0}$, it holds that $\bar{\mathbf{U}}^N(t)$ reaches its maximum componentwise value at the boundary $\partial\Omega^N \times [0, T] \cup \Omega^N \times \{0\}$.

The proof of this result is similar to the proof of the semidiscrete maximum principle stated in [6]. From Lemma 6, the next result immediately follows.

Lemma 7. If $[\mathbf{f}(x, t)]_{\Omega^N} \geq \mathbf{0}$, $\mathbf{g}_0(t) \geq \mathbf{0}$, $\mathbf{g}_1(t) \geq \mathbf{0}$, and $[\varphi(x)]_{\Omega^N} \geq \mathbf{0}$, then $\bar{\mathbf{U}}^N(t) \geq \mathbf{0}$.

Using now a well known barrier-function technique, see [26] for instance, the following result can be proved.

Lemma 8 (Uniform stability). The unique solution of problem (33) satisfies the uniform bound

$$\|\bar{\mathbf{U}}^N(t)\|_{\bar{\Omega}^N \times [0, T]} \leq \max\{\|[\varphi(x)]_{\Omega^N}\|_{\Omega^N}, \|\mathbf{g}_0(t)\|_{[0, T]}, \|\mathbf{g}_1(t)\|_{[0, T]}\} + \frac{1}{\beta} \|[\mathbf{f}(x, t)]_{\Omega^N}\|_{\Omega^N \times [0, T]}.$$

From Taylor expansions, we know that for any sufficiently smooth continuous function $z(x, t)$, it holds

$$\left| \left(\frac{\partial^2}{\partial x^2} - \delta_x^2 \right) z(x_i, t) \right| \leq C \max_{\xi \in [x_{i-1}, x_{i+1}]} \left| \frac{\partial^2 z}{\partial x^2}(\xi, t) \right|, \tag{36}$$

$$\left| \left(\frac{\partial^2}{\partial x^2} - \delta_x^2 \right) z(x_i, t) \right| \leq C(x_{i+1} - x_{i-1}) \max_{\xi \in [x_{i-1}, x_{i+1}]} \left| \frac{\partial^3 z}{\partial x^3}(\xi, t) \right|, \tag{37}$$

$$\left| \left(\frac{\partial}{\partial x} - D_x^- \right) z(x_i, t) \right| \leq C(x_{i+1} - x_{i-1}) \max_{\xi \in [x_{i-1}, x_i]} \left| \frac{\partial^2 z}{\partial x^2}(\xi, t) \right|, \tag{38}$$

$$\left| \left(\frac{\partial}{\partial x} - D_x^- \right) z(x_i, t) \right| \leq C \max_{\xi \in [x_{i-1}, x_i]} \left| \frac{\partial z}{\partial x}(\xi, t) \right|. \tag{39}$$

The main result in this section proves the uniform convergence of the spatial discretization.

Theorem 1. Under the previous smoothness assumptions for \mathbf{u} , the error associated with the spatial discretization on the Shishkin mesh satisfies

$$\|[\mathbf{u}(x, t)]_N - \mathbf{U}^N(t)\|_{\Omega^N} \leq CN^{-1} \ln N, \quad \forall t \in [0, T], \tag{40}$$

where C is independent of ϵ and N , and therefore the spatial discretization is an almost first order uniformly convergent scheme.

Proof. We only show the details when $\sigma_{\epsilon_2} = \sigma_0 \epsilon_2 \ln N$, $\sigma_{\epsilon_1} = \sigma_0 \epsilon_1 \ln N$, which is the most interesting case. The other simpler cases can be studied in similar way as in [2].

Following to the continuous problem, we decompose the numerical solution in the form $\mathbf{U}^N(t) = \mathbf{V}^N(t) + \mathbf{W}^N(t)$, where the regular component $\mathbf{V}^N(t)$ is the solution of the problem

$$\begin{cases} \frac{d\mathbf{V}^N}{dt}(t) + \mathcal{L}_\epsilon^N(t)\bar{\mathbf{V}}^N(t) = [\mathbf{f}(x, t)]_{\Omega^N}, & \text{in } \Omega^N \times [0, T], \\ \mathbf{V}_0^N(t) = \mathbf{v}(0, t), & \text{in } [0, T], \\ \mathbf{V}_1^N(t) = \mathbf{v}(1, t), & \text{in } [0, T], \\ \mathbf{V}^N(0) = [\varphi(x)]_{\Omega^N}, \end{cases} \tag{41}$$

and the singular component $\mathbf{W}^N(t)$ is the solution of the problem

$$\begin{cases} \frac{d\mathbf{W}^N}{dt}(t) + \mathcal{L}_\epsilon^N(t)\bar{\mathbf{W}}^N(t) = \mathbf{0}, & \text{in } \Omega^N \times [0, T], \\ \mathbf{W}_0^N(t) = \mathbf{w}(0, t), & \text{in } [0, T], \\ \mathbf{W}_1^N(t) = \mathbf{w}(1, t), & \text{in } [0, T], \\ \mathbf{W}^N(0) = \mathbf{0} & \text{in } \Omega^N. \end{cases} \tag{42}$$

Then, it trivially holds

$$\|[\mathbf{u}(x, t)]_N - \mathbf{U}^N(t)\|_{\Omega^N} \leq \|[\mathbf{v}(x, t)]_N - \mathbf{V}^N(t)\|_{\Omega^N} + \|[\mathbf{w}(x, t)]_N - \mathbf{W}^N(t)\|_{\Omega^N}$$

and we analyze the error of the regular and the singular components separately.

We remember that the local error at any time $t \in [0, T]$, at the grid point $x_i \in \overline{\Omega}_N$, $i = 1, \dots, N - 1$, is given by

$$v_{i,N,\mathbf{u}}(t) \equiv \mathbf{L}_\varepsilon \mathbf{u}(x_i, t) - (\mathbf{L}_\varepsilon^N[\mathbf{u}(x, t)]_N)_i.$$

Taking into account that the contribution of the time derivatives to the local error is zero, we deduce that

$$v_{i,N,\mathbf{u}}(t) = \mathcal{L}_\varepsilon(t)\mathbf{u}(x_i, t) - (\mathcal{L}_\varepsilon^N[\mathbf{u}(x, t)]_N)_i$$

For the regular component, using (37), (38) and the estimates (10) for the derivatives, we obtain $|v_{i,N,\mathbf{v}}(t)| \leq \mathbf{C}N^{-1}$ and from Lemma 7 it follows

$$|\mathbf{v}(x_i, t) - \mathbf{V}_i^N(t)| \leq \mathbf{C}N^{-1}. \tag{43}$$

For the singular component we distinguish several cases depending on the location of the mesh point x_i , $i = 1, 2, \dots, N - 1$.

Case 1: We assume that $x_i \in (0, 1 - \sigma_{\varepsilon_2}]$. As it is usual, in this case the error is bounded directly using that

$$|\mathbf{w}(x_i, t) - \mathbf{W}_i^N(t)| \leq |\mathbf{w}(x_i, t)| + |\mathbf{W}_i^N(t)|.$$

From (19) we obtain

$$|\mathbf{w}(x_i, t)| \leq \mathbf{C}e^{-\beta\sigma_{\varepsilon_2}/\varepsilon_2} \leq \mathbf{C}N^{-2}.$$

On the other hand, we define the barrier function

$$\psi_{\varepsilon_2,i} = \prod_{j=i+1}^N \left(1 + \frac{\beta h_j}{2\varepsilon_2}\right)^{-1}, \quad i = 1, 2, \dots, N - 1,$$

and $\Psi_{\varepsilon_2,i} = (\psi_{\varepsilon_2,i}, \psi_{\varepsilon_2,i})^T$. Then, we can prove

$$\mathbf{L}_\varepsilon^N[\Psi_{\varepsilon_2,i}] \geq \mathbf{C} \frac{\psi_{\varepsilon_2,i}}{2\varepsilon_2 + \beta h_{i+1}}.$$

Using that $\psi_{\varepsilon_2,i} \geq e^{-\frac{\beta x_i}{2\varepsilon_2}}$, we deduce $|\mathbf{W}_i^N(t)| \leq \mathbf{C}N^{-2}$ (see [2] for more details where same idea was used in this case).

From previous estimates, in this case we obtain

$$|\mathbf{w}(x_i, t) - \mathbf{W}_i^N(t)| \leq \mathbf{C}N^{-2}. \tag{44}$$

Case 2: We assume that $x_i \in [1 - \sigma_{\varepsilon_1}, 1)$. In this case we define a new barrier function, given by

$$\psi_{\varepsilon_1,i} = \prod_{j=i+1}^N \left(1 + \frac{\beta h_j}{2\varepsilon_1}\right)^{-1}, \quad i = 1, 2, \dots, N - 1.$$

Then, using the remainder of Taylor expansion in integral form, we have

$$\begin{aligned} \left| \mathcal{L}_{\varepsilon,1}^N(t) \left(\mathbf{w}(x_i, t) - \mathbf{W}_i^N(t) \right) \right| &\leq \mathbf{C} \int_{x_{i-1}}^{x_i-1} \left(\varepsilon_1 \left| \frac{\partial^3 w_1}{\partial x^3} \right| + \left| \frac{\partial^2 w_1}{\partial x^2} \right| \right) (s, t) ds \leq \\ &\mathbf{C} \left(\varepsilon_1^{-1} \exp(-\beta(1-x_i)/\varepsilon_1) \sinh(\beta h_{\varepsilon_1}/\varepsilon_1) + \exp(-\beta(1-x_i)/\varepsilon_2) \sinh(\beta h_{\varepsilon_1}/\varepsilon_2) \right) \leq \\ &\mathbf{C} \left(\varepsilon_1^{-1} N^{-1} \ln N \psi_{\varepsilon_1,i} + N^{-1} \ln N \psi_{\varepsilon_2,i} \right). \end{aligned}$$

Similarly, we can prove

$$\begin{aligned} \left| \mathcal{L}_{\varepsilon,2}^N(t) \left(\mathbf{w}(x_i, t) - \mathbf{W}_i^N(t) \right) \right| &\leq \mathbf{C} \int_{x_{i-1}}^{x_i-1} \left(\varepsilon_2 \left| \frac{\partial^3 w_2}{\partial x^3} \right| + \left| \frac{\partial^2 w_2}{\partial x^2} \right| \right) (s, t) ds \leq \\ &\mathbf{C} \left(N^{-1} \ln N \psi_{\varepsilon_1,i} + \varepsilon_2^{-1} N^{-1} \ln N \psi_{\varepsilon_2,i} \right). \end{aligned}$$

Then, it holds

$$|v_{i,N,\mathbf{w}}(t)| \leq \mathbf{C} \left(\varepsilon_1^{-1} N^{-1} \ln N \psi_{\varepsilon_1,i} + \varepsilon_2^{-1} N^{-1} \ln N \psi_{\varepsilon_2,i} \right).$$

Case 3: We assume that $x_i \in (1 - \sigma_{\varepsilon_2}, 1 - \sigma_{\varepsilon_1})$. In this case we use ideas given in [2,21]. Let x^* the value where

$$\varepsilon_1^{-1} \exp(-\beta(1 - x_i)/\varepsilon_1) + \varepsilon_2^{-1} \exp(-\beta(1 - x_i)/\varepsilon_2),$$

attains the maximum in the interval $[x_{i-1}, x_{i+1}]$. Now we must distinguish two subcases; in the first one we assume that it holds

$$\varepsilon_1^{-1} \exp(-\beta(1 - x_i)/\varepsilon_1) \leq \varepsilon_2^{-1} \exp(-\beta(1 - x_i)/\varepsilon_2). \tag{45}$$

Then, using (37) and (38) we have

$$\begin{aligned} \left| \mathcal{L}_{\varepsilon,1}^N(t) \left(\mathbf{w}(x_i, t) - \mathbf{W}_i^N(t) \right) \right| &\leq C(x_{i+1} - x_{i-1}) \max_{\xi \in [x_{i-1}, x_{i+1}]} \left(\varepsilon_1 \left| \frac{\partial^3 w_1}{\partial x^3} \right| + \left| \frac{\partial^2 w_1}{\partial x^2} \right| \right) (\xi, t) \leq \\ &Ch_{\varepsilon_2} \left(\varepsilon_1^{-2} \exp(-\beta(1 - x^*)/\varepsilon_1) + \varepsilon_2^{-2} \exp(-\beta(1 - x^*)/\varepsilon_2) \right) \leq \\ &C\varepsilon_2^{-1} N^{-1} \ln N \exp(-\beta(1 - x_i)/\varepsilon_2) \exp(\beta h_{\varepsilon_2}/\varepsilon_2) \leq \\ &\varepsilon_2^{-1} N^{-1} \ln N \psi_{\varepsilon_2,i}. \end{aligned}$$

Similarly, we can prove

$$\begin{aligned} \left| \mathcal{L}_{\varepsilon,2}^N(t) \left(\mathbf{w}(x_i, t) - \mathbf{W}_i^N(t) \right) \right| &\leq C(x_{i+1} - x_{i-1}) \max_{\xi \in [x_{i-1}, x_{i+1}]} \left(\varepsilon_2 \left| \frac{\partial^3 w_2}{\partial x^3} \right| + \left| \frac{\partial^2 w_2}{\partial x^2} \right| \right) (\xi, t) \leq \\ &Ch_{\varepsilon_2} \left(\varepsilon_1^{-1} \exp(-\beta(1 - x^*)/\varepsilon_1) + \varepsilon_2^{-2} \exp(-\beta(1 - x^*)/\varepsilon_2) \right) \leq \\ &C\varepsilon_2^{-1} N^{-1} \ln N \psi_{\varepsilon_2,i}. \end{aligned}$$

Then, in this subcase it holds

$$|v_{i,N,\mathbf{w}}(t)| \leq C\varepsilon_2^{-1} N^{-1} \ln N \psi_{\varepsilon_2,i}.$$

In the last case, which is not considered in [2], we assume that (45) does not hold. Then, using (36) and (39) we have

$$\begin{aligned} \left| \mathcal{L}_{\varepsilon,1}^N(t) \left(\mathbf{w}(x_i, t) - \mathbf{W}_i^N(t) \right) \right| &\leq C \max_{\xi \in [x_{i-1}, x_{i+1}]} \left(\varepsilon_1 \left| \frac{\partial^2 w_1}{\partial x^2} \right| + \left| \frac{\partial w_1}{\partial x} \right| \right) (\xi, t) \leq \\ &C \left(\varepsilon_1^{-1} \exp(-\beta(1 - x^*)/\varepsilon_1) + \exp(-\beta(1 - x^*)/\varepsilon_2) \right) \leq \\ &C\varepsilon_1^{-1} \exp(-\beta\sigma_{\varepsilon_1}/(2\varepsilon_1)) \exp(-\beta(1 - x_{i+1})/(2\varepsilon_1)) \leq C\varepsilon_1^{-1} N^{-1} \ln N \psi_{\varepsilon_1,i+1}. \end{aligned}$$

Similarly, we can prove

$$\begin{aligned} \left| \mathcal{L}_{\varepsilon,2}^N(t) \left(\mathbf{w}(x_i, t) - \mathbf{W}_i^N(t) \right) \right| &\leq C \max_{\xi \in [x_{i-1}, x_{i+1}]} \left(\varepsilon_2 \left| \frac{\partial^2 w_2}{\partial x^2} \right| + \left| \frac{\partial w_2}{\partial x} \right| \right) (\xi, t) \leq \\ &C\varepsilon_2^{-1} \exp(-\beta(1 - x_{i+1})/\varepsilon_2) \leq \\ &C\varepsilon_1^{-1} \exp(-\beta\sigma_{\varepsilon_1}/(2\varepsilon_1)) \exp(-\beta(1 - x_{i+1})/(2\varepsilon_1)) \leq C\varepsilon_1^{-1} N^{-1} \ln N \psi_{\varepsilon_1,i+1}. \end{aligned}$$

Then, in this subcase it holds

$$|v_{i,N,\mathbf{w}}(t)| \leq C \left(\varepsilon_1^{-1} N^{-1} \ln N \psi_{\varepsilon_1,i+1} \right).$$

To finish the proof we consider the barrier function

$$\psi_{\varepsilon_1,\varepsilon_2,i} = CN^{-1} \ln N (\varepsilon_1^{-1} \psi_{\varepsilon_1,i+1} + \varepsilon_2^{-1} \psi_{\varepsilon_2,i}), \quad i = 1, 2, \dots, N - 1,$$

and $\Psi_{\varepsilon_1,\varepsilon_2,i} = (\psi_{\varepsilon_1,\varepsilon_2,i}, \psi_{\varepsilon_1,\varepsilon_2,i})^T$; using the maximum principle we can obtain

$$|\mathbf{w}(x_i, t) - \mathbf{W}_i^N(t)| \leq CN^{-1} \ln N. \tag{46}$$

Then, from (43), (44) and (46) the required result follows. \square

4. The fully discrete scheme: uniform convergence

In this section we describe the numerical algorithm which we propose to solve efficiently the continuous problem (1). Our method is the result of applying an appropriate time integrator to the semidiscrete problems (33).

Let us consider, for simplicity, a constant time step $\tau = T/M$; we denote $\mathbf{U}^{N,m} \equiv (\mathbf{U}_i^{N,m})$, $i = 1, \dots, N - 1$, where $\mathbf{U}_i^{N,m} \equiv (U_{1,i}^{N,m}, U_{2,i}^{N,m})^T$ are the numerical approaches of $\mathbf{u}(x_i, t_m)$, $i = 1, \dots, N - 1$ at $t_m = m\tau$, for $m = 0, 1, \dots, M$ and let us denote $\bar{\mathbf{U}}^{N,m} \equiv (\mathbf{U}_i^{N,m})$, $i = 0, \dots, N$. Using these notations, the fully discrete scheme is given by

Initialize
 $\bar{\mathbf{U}}^{N,0} = [\boldsymbol{\varphi}]_{\bar{\Omega}^N}$,
 For $m = 0, 1, \dots, M - 1$,
 First half step
 $U_{2,i}^{N,m+1/2} = U_{2,i}^{N,m}, i = 0, \dots, N$,

$$\begin{cases} U_{1,0}^{N,m+1/2} = g_{1,0}(t_{m+1}), \\ \frac{U_{1,i}^{N,m+1/2} - U_{1,i}^{N,m}}{\tau} + (\mathcal{L}_{\boldsymbol{\epsilon}}^N(t_{m+1})\bar{\mathbf{U}}^{N,m+1/2})_{1,i} = f_1(x_i, t_{m+1}), i = 1, \dots, N - 1, \\ U_{1,N}^{N,m+1/2} = g_{1,1}(t_{m+1}), \end{cases} \tag{47}$$

 Second half step
 $U_{1,i}^{N,m+1} = U_{1,i}^{N,m+1/2}, i = 0, \dots, N$,

$$\begin{cases} U_{2,0}^{N,m+1} = g_{2,0}(t_{m+1}), \\ \frac{U_{2,i}^{N,m+1} - U_{2,i}^{N,m+1/2}}{\tau} + (\mathcal{L}_{\boldsymbol{\epsilon}}^N(t_{m+1})\bar{\mathbf{U}}^{N,m+1})_{2,i} = f_2(x_i, t_{m+1}), i = 1, \dots, N - 1, \\ U_{2,n}^{N,m+1} = g_{2,1}(t_{m+1}). \end{cases}$$

Observe that in the half steps of (47), only tridiagonal linear systems are involved to obtain the numerical approaches $\mathbf{U}^{N,*}$. Because of that, we obtain a remarkable cost reduction with our method, if we compare it with classical implicit methods (see, for example, [12]).

Next, we describe the main theoretical results of this time integration process which take an important role in the analysis of the uniform and unconditional convergence of our method, formulated and proven in the last theorem of this section.

4.1. Analysis of time integration: uniform stability

Theorem 2. The linear systems involved in (47) are associated with tridiagonal matrices of the form

$$A_{N,k} \equiv I_N + \tau \mathcal{L}_{\boldsymbol{\epsilon},k}^N, k = 1, 2,$$

which are inverse positive and satisfy

$$\|(A_{N,k})^{-1}\|_{\infty} \leq 1, k = 1, 2; \tag{48}$$

therefore, (47) has a unique solution.

Notice that the non zero coefficients of i -th row of the tridiagonal matrix $\mathcal{L}_{\boldsymbol{\epsilon},k}^N$ are $r_{k,i}^-, r_{k,i}^c + a_{kk}(x_i, t_{m+1}), r_{k,i}^+$, which are defined in (35). From this result, using a similar process to this one in the proof of Corollary 1 of [6], it is proven the following contractive behavior of the method.

Theorem 3 (Uniform stability). Two solutions of (47) obtained with different initial conditions, $\mathbf{U}^{N,0}$ and $\tilde{\mathbf{U}}^{N,0}$, satisfy

$$\|\mathbf{U}^{N,m+1} - \tilde{\mathbf{U}}^{N,m+1}\|_{\Omega_N} \leq \|\mathbf{U}^{N,m} - \tilde{\mathbf{U}}^{N,m}\|_{\Omega_N}. \tag{49}$$

4.2. Analysis of time integration: uniform consistency

To complete the uniform convergence of the time integration process, first we study its uniform consistency. To do this, we introduce the local errors in time $e^{N,m}$, at times t_m , which are defined by

$$e^{N,m} = \mathbf{U}^N(t_m) - \hat{\mathbf{U}}^{N,m},$$

being $\hat{\mathbf{U}}^{N,m}$ the result of the m -th step of scheme (47), if we change $\bar{\mathbf{U}}^{N,m-1}$ by $\bar{\mathbf{U}}^N(t_{m-1})$. By doing similar calculations to the proof of Theorem 6 of [6], the following result can be obtained.

Theorem 4 (Uniform consistency). Under the assumptions made for the data of problem (1), it holds

$$\|e^{N,m}\|_{\Omega_N} \leq CM^{-2}, \quad \forall \tau \in (0, \tau_0] \text{ and } m = 1, 2, \dots, M. \tag{50}$$

Now, combining the two main results of the preceding short subsections, we are ready to prove that the time integration process is uniformly convergent of first order.

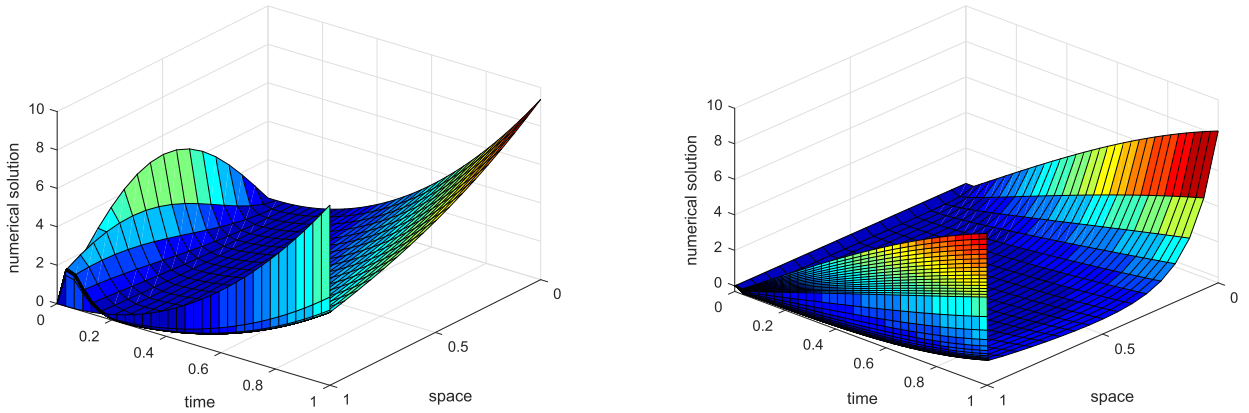


Fig. 1. Components u_1 (left) and u_2 (right) of example (53) for $\varepsilon_1 = 10^{-4}, \varepsilon_2 = 10^{-3}$ with $N = 48, M = 32$.

4.3. Analysis of time integration: uniform convergence

Let us introduce the global errors in time, at times t_m , as $(\bar{\mathbf{U}}^N(t_m) - \mathbf{U}^{N,m})$ for $m = 1, \dots, M$. They can be bounded in the form

$$\|\bar{\mathbf{U}}^N(t_m) - \mathbf{U}^{N,m}\|_{\Omega^N} \leq \|\mathbf{e}^{N,m}\|_{\Omega^N} + \|\hat{\mathbf{U}}^{N,m} - \mathbf{U}^{N,m}\|_{\Omega^N}.$$

Now, using the stability result (49), we obtain

$$\|\bar{\mathbf{U}}^N(t_m) - \mathbf{U}^{N,m}\|_{\Omega^N} \leq \|\mathbf{e}^{N,m}\|_{\Omega^N} + \|\bar{\mathbf{U}}^N(t_{m-1}) - \mathbf{U}^{N,m-1}\|_{\Omega^N}.$$

Applying m times this recurrence and the bounds (50) for the local error, it is straightforward to prove that

$$\|\bar{\mathbf{U}}^N(t_m) - \mathbf{U}^{N,m}\|_{\Omega^N} \leq \sum_{i=1}^m \|\mathbf{e}^{N,i}\|_{\Omega^N} \leq CM^{-1}. \tag{51}$$

Therefore, the time integration process is uniformly convergent of first order.

Combining this result and the uniform convergence of the spatial discretization process, we are ready to state the main uniform convergence result of the paper.

Theorem 5 (Uniform convergence). Assuming that $\mathbf{u} \in C^{4,2}(\bar{Q})$, the global error associated to the numerical method defined by (47) on the Shishkin mesh defined in (32) satisfies

$$\max_{0 \leq m \leq M} \|\bar{\mathbf{U}}^{N,m} - [\mathbf{u}(x, t_m)]\|_{\Omega^N} \leq C(N^{-1} \ln N + M^{-1}), \tag{52}$$

where the constant C is independent of the diffusion parameter ε and the discretization parameters N and M .

5. Numerical results

In this section we show the numerical results obtained with the algorithm proposed in this paper to solve successfully some problems of type (1). The data which we have chosen for the first numerical test are:

$$\begin{aligned} \mathbf{A} &= \begin{pmatrix} 10 - x^2 - t^2 & -(1 + x^2 + t^2) \\ -xte^x & 10 + 3 \cos(x + t) \end{pmatrix}, \quad \mathbf{B} = \begin{pmatrix} 10 + 3 \sin(x) & 0 \\ 0 & 1 + x(1 - x^2) \end{pmatrix}, \\ \mathbf{f}(x, t) &= (5t^2 \sin(x + t), 2t \sin(t)e^{xt})^T, \\ \mathbf{g}_0(t) &= (10t^2, 10t^2)^T, \quad \mathbf{g}_1(t) = (10 \sin(t), 10 \sin(t))^T, \quad \boldsymbol{\varphi}(x) = (5 \sin(\pi x), 0)^T, \end{aligned} \tag{53}$$

and $T = 1$. Fig. 1 displays the numerical solution for $\varepsilon_1 = 10^{-4}, \varepsilon_2 = 10^{-3}$. From it, we clearly see the presence of regular boundary layers at the outflow boundary.

To observe more in detail the overlapping boundary layers at $x = 1$, Fig. 2 displays both components at the final time $T = 1$; the graph of the right hand side contains a zoom of the boundary layer region. In it, it is seen that the layer associated to the first component is sharper than the associated to the second one.

As the exact solution of this example is unknown, to approximate the maximum errors for each component $u_k, k = 1, 2$, given by

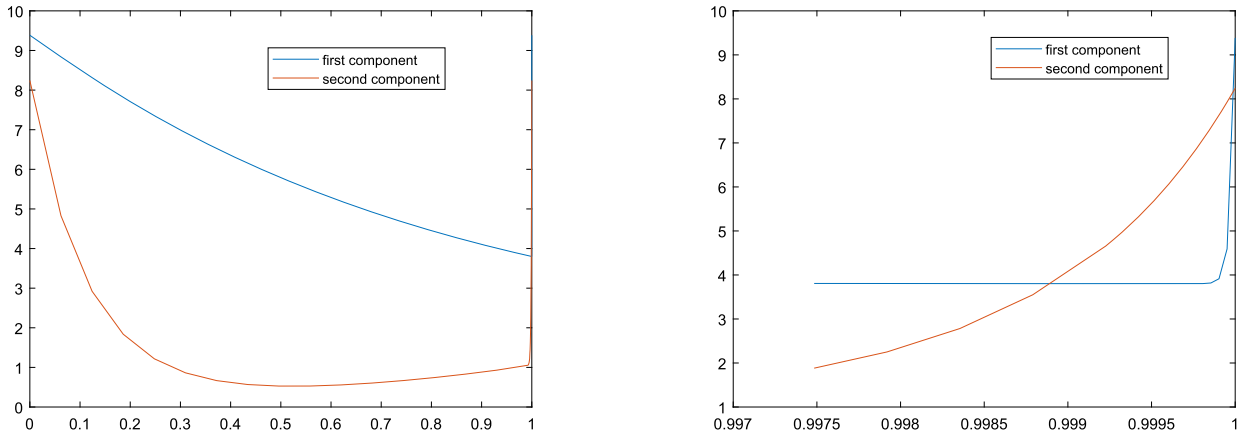


Fig. 2. Components of example (53) for $\varepsilon_1 = 10^{-4}$, $\varepsilon_2 = 10^{-3}$ at $T = 1$.

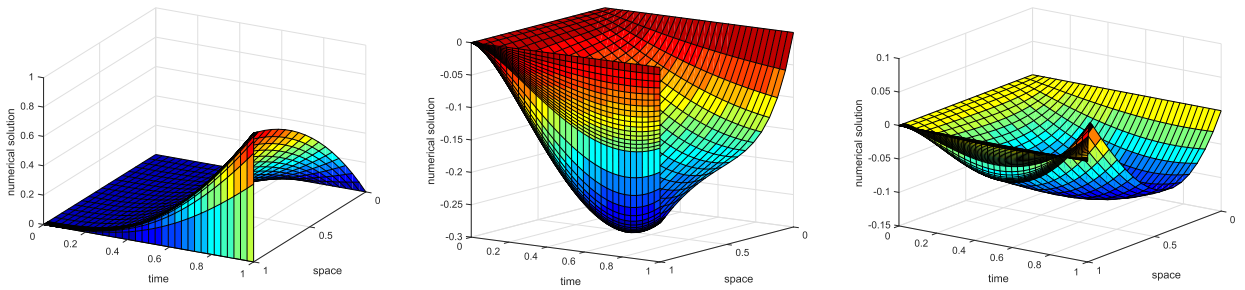


Fig. 3. Components of example (56) for $\varepsilon_1 = 10^{-5}$, $\varepsilon_2 = 10^{-4}$, $\varepsilon_3 = 10^{-3}$, with $N = 64$, $M = 32$ (left u_1 , center u_2 , right u_3).

$$\max_{0 \leq m \leq M} \max_{0 \leq i \leq N} |U_{N,i,k}^m - u_k(x_i, t_m)|, k = 1, 2,$$

we use a variant of the double-mesh principle (see [8] for instance), i.e., we calculate

$$d_{\varepsilon,k}^{N,M} = \max_{0 \leq m \leq M} \max_{0 \leq i \leq N} |U_{N,i,k}^m - \widehat{U}_{2N,2i,k}^{2m}|, d_k^{N,M} = \max_{\varepsilon} d_{\varepsilon,k}^{N,M}, k = 1, 2, \tag{54}$$

where $\{\widehat{U}_{2N}^{2m}\}$ is the numerical solution on a finer mesh $\{(\widehat{x}_j, \widehat{t}_m)\}$ that consists of the mesh points of the coarse mesh and their midpoints. From the double-mesh differences computed in (54), we obtain the corresponding orders of convergence, given by

$$p_k = \log(d_{\varepsilon,k}^{N,M} / d_{\varepsilon,k}^{2N,2M}) / \log 2, p_k^{uni} = \log(d_k^{N,M} / d_k^{2N,2M}) / \log 2, k = 1, 2. \tag{55}$$

Table 1 shows the maximum errors and the orders of convergence for some values of ε_2 , taking $\sigma_0 = 2$ in (30) and $M = N/2$; for each value of ε_2 , the diffusion parameter ε_1 is in the set $R = \{\varepsilon_1 | \varepsilon_1 = \varepsilon_2, 2^{-2}\varepsilon_2, \dots, 2^{-32}\varepsilon_2\}$. For each value of ε_2 , the first and second rows correspond to the first component and the third and the fourth ones to the second one. From this table, we observe the almost first order of uniform convergence according to the theoretical results. This fact indicates that, from a numerical point of view, the errors associated to the spatial discretization dominate in the global errors.

To show that the splitting technique can be extended successfully to systems with more components, we consider a second example where the system of partial differential equations has three coupled equations and the unknown solution has three components. The data of this problem are given by

$$\mathbf{A} = \begin{pmatrix} 5 + xt & -(x^2 + t^2) & -(2 + xt) \\ -5xte^{-x} & 6 + \cos(xt) & -\sin(x + t) \\ -3xe^{-t} & -(xt + \sin(xt)) & 5(x + 1)e^{-xt} \end{pmatrix}, \mathbf{B} = \begin{pmatrix} 5 + x \sin(x) & 0 & 0 \\ 0 & 1 + x^2 & 0 \\ 0 & 0 & 3 - x \cos(x) \end{pmatrix}, \tag{56}$$

$$\mathbf{f}(\mathbf{x}, t) = (10t^2 \sin(x + t), -2(1 - e^{-t})e^x, -3t \cos(x + t))^T, \mathbf{g}_0 = \mathbf{g}_1 = \boldsymbol{\varphi} = \mathbf{0},$$

and $T = 1$, for which again the exact solution is unknown. Fig. 3 displays the numerical approximation for the three components, showing again the overlapping boundary layers at $x = 1$.

As in the previous example, to see more clearly the overlapping boundary layers at $x = 1$, Fig. 4 displays the components at the final time $T = 1$; from it, we can observe that the layer associated to the first component is sharper than the associated to the second one and this one is sharper than the associated one to the third component.

Table 1
Maximum errors and orders of convergence for example (53).

ε_2	$N = 48$	$N = 96$	$N = 192$	$N = 384$	$N = 768$	$N = 1536$
2^{-6}	5.7355E-1	5.3868E-1	4.9110E-1	3.6168E-1	2.4754E-1	1.5576E-1
	0.0905	0.1334	0.4413	0.5470	0.6683	
	3.0874E-1	1.6282E-1	9.5811E-2	5.6207E-2	3.2010E-2	1.7871E-2
	0.9231	0.7650	0.7695	0.8122	0.8409	
2^{-8}	5.8292E-1	5.4407E-1	4.9470E-1	3.6390E-1	2.4905E-1	1.5665E-1
	0.0995	0.1372	0.4430	0.5471	0.6688	
	3.9442E-1	2.2502E-1	1.2104E-1	6.2643E-2	3.3959E-2	1.8941E-2
	0.8097	0.8946	0.9502	0.8834	0.8422	
2^{-10}	5.8624E-1	5.4575E-1	4.9577E-1	3.6457E-1	2.4949E-1	1.5699E-1
	0.1032	0.1386	0.4435	0.5472	0.6683	
	4.1851E-1	2.4662E-1	1.3500E-1	7.0777E-2	3.6279E-2	1.9359E-2
	0.7630	0.8694	0.9316	0.9641	0.9061	
2^{-12}	5.8713E-1	5.4631E-1	4.9605E-1	3.6474E-1	2.4961E-1	1.5702E-1
	0.1040	0.1392	0.4436	0.5472	0.6688	
	4.2472E-1	2.5239E-1	1.3880E-1	7.3116E-2	3.7569E-2	1.9481E-2
	0.7508	0.8627	0.9247	0.9607	0.9474	
...	
2^{-24}	5.8743E-1	5.4650E-1	4.9615E-1	3.6480E-1	2.4966E-1	1.5702E-1
	0.1042	0.1394	0.4437	0.5471	0.6690	
	4.2680E-1	2.5435E-1	1.4009E-1	7.3918E-2	3.8013E-2	1.9408E-2
	0.7468	0.8604	0.9224	0.9595	0.9698	
$e_1^{N,M}$	5.8743E-1	5.4650E-1	4.9615E-1	3.6480E-1	2.4966E-1	1.5708E-1
p_1^{uni}	0.1042	0.1394	0.4437	0.5471	0.6685	
$e_2^{N,M}$	4.2680E-1	2.5435E-1	1.4009E-1	7.3918E-2	3.8013E-2	1.9521E-2
p_2^{uni}	0.7468	0.8604	0.9224	0.9595	0.9614	

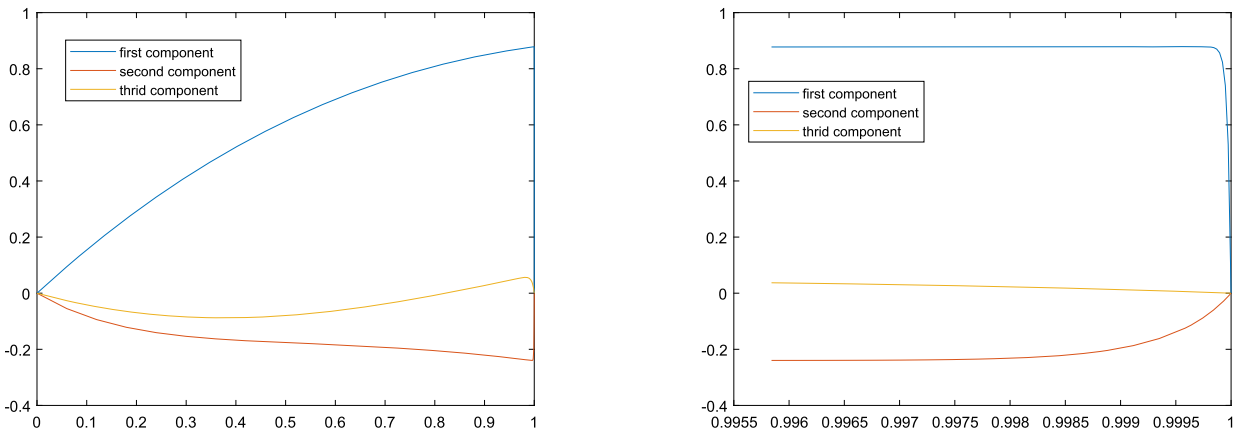


Fig. 4. Components of example (56) for $\varepsilon_1 = 10^{-5}$, $\varepsilon_2 = 10^{-4}$, $\varepsilon_3 = 10^{-3}$ at $T = 1$.

To obtain the numerical solution, we have used the same ideas as in [6] for extend our splitting technique to systems with more components. First, following to [18] we construct the appropriate piecewise uniform Shishkin mesh to solve a system with three equations which may have three different diffusion parameters. For that, we define the transition parameters

$$\sigma_{\varepsilon_3} = \min \{3/4, \sigma_0 \varepsilon_3 \ln N\}, \quad \sigma_{\varepsilon_2} = \min \{2\sigma_{\varepsilon_3}/3, \sigma_0 \varepsilon_2 \ln N\}, \quad \sigma_{\varepsilon_1} = \min \{\sigma_{\varepsilon_2}/2, \sigma_0 \varepsilon_1 \ln N\}, \tag{57}$$

where N is a positive integer multiple of 4; then, the grid points are given by

$$x_i = \begin{cases} iH, & i = 0, \dots, N/4, \\ x_{N/4} + (i - N/4)h_{\varepsilon_3}, & i = N/4 + 1, \dots, N/2, \\ x_{N/2} + (i - N/2)h_{\varepsilon_2}, & i = N/2 + 1, \dots, 3N/4, \\ x_{3N/4} + (i - 3N/4)h_{\varepsilon_1}, & i = 3N/4 + 1, \dots, N, \end{cases}$$

Table 2
Maximum errors and orders of convergence for example (56).

ε_3	$N = 32$	$N = 64$	$N = 128$	$N = 256$	$N = 512$
2^{-6}	8.7654E-2	6.9700E-2	4.7361E-2	3.2337E-2	2.0392E-2
	0.3307	0.5574	0.5505	0.6652	
	1.5112E-2	1.0158E-2	6.5394E-3	3.9704E-3	2.3217E-3
	0.5731	0.6354	0.7199	0.7741	
	1.0400E-2	5.4425E-3	2.7760E-3	1.3944E-3	7.7145E-4
	0.9342	0.9712	0.9933	0.8540	
2^{-8}	8.8799E-2	7.0251E-2	4.7756E-2	3.2506E-2	2.0500E-2
	0.3380	0.5568	0.5550	0.6650	
	1.4962E-2	1.0073E-2	6.4828E-3	3.9401E-3	2.3044E-3
	0.5708	0.6359	0.7184	0.7738	
	1.0879E-2	5.7790E-3	2.9761E-3	1.5089E-3	8.0340E-4
	0.9126	0.9574	0.9799	0.9093	
2^{-10}	8.9115E-2	7.0406E-2	4.7870E-2	3.2554E-2	2.0532E-2
	0.3400	0.5566	0.5563	0.6650	
	1.4909E-2	1.0046E-2	6.4634E-3	3.9294E-3	2.2981E-3
	0.5695	0.6363	0.7180	0.7738	
	1.0994E-2	5.8648E-3	3.0268E-3	1.5380E-3	8.1200E-4
	0.9066	0.9543	0.9767	0.9215	
...
2^{-24}	8.9221E-2	7.0459E-2	4.7908E-2	3.2571E-2	2.0543E-2
	0.3406	0.5565	0.5567	0.6649	
	1.3926E-2	9.7226E-3	6.1977E-3	3.7755E-3	2.2114E-3
	0.5184	0.6496	0.7151	0.7718	
	1.1032E-2	5.8932E-3	3.0436E-3	1.5479E-3	7.8067E-4
	0.9046	0.9533	0.9754	0.9876	
$d_1^{N,M}$	8.9222E-2	7.0459E-2	4.7908E-2	3.2571E-2	2.0543E-2
p_1^{uni}	0.3406	0.5565	0.5567	0.6649	
$d_2^{N,M}$	1.5112E-2	1.0158E-2	6.5394E-3	3.9704E-3	2.3217E-3
p_2^{uni}	0.5731	0.6354	0.7199	0.7741	
$d_3^{N,M}$	1.1032E-2	5.8932E-3	3.0436E-3	1.5479E-3	8.1448E-4
p_3^{uni}	0.9046	0.9533	0.9754	0.9264	

where $H = 4(1 - \sigma_{\varepsilon_3})/N$, $h_{\varepsilon_3} = 4(\sigma_{\varepsilon_3} - \sigma_{\varepsilon_2})/N$, $h_{\varepsilon_2} = 4(\sigma_{\varepsilon_2} - \sigma_{\varepsilon_1})/N$, $h_{\varepsilon_1} = 4\sigma_{\varepsilon_1}/N$. Secondly, we semidiscretize in space this problem using again the simple upwind finite difference scheme on this mesh and, finally, we integrate in time the Initial Value Problems coming from the spatial discretization, by using the fractional implicit Euler method, with three fractional steps, joint to a splitting in three components (see [6] for full details) to obtain the numerical algorithm.

To estimate the maximum errors we use again the double mesh principle. Table 2 shows the maximum errors for some values of ε_3 taking ε_2 in the set $R_2 = \{\varepsilon_2 | \varepsilon_2 = \varepsilon_3, 2^{-2}\varepsilon_3, \dots, 2^{-28}\varepsilon_3\}$ and ε_1 in the set $R_1 = \{\varepsilon_1 | \varepsilon_1 = \varepsilon_2, 2^{-2}\varepsilon_2, \dots, 2^{-32}\varepsilon_2\}$, $\sigma_0 = 1$ in (57) and $M = N/2$. For each value of ε_3 , the first and second rows correspond to the first component, the third and the fourth ones to the second component and the fifth and sixth ones to the third component. From it, we observe again the almost first order of uniform convergence of the numerical algorithm.

One of the most important properties of our method, in comparison with other uniformly convergent classical methods used to solve parabolic singularly perturbed systems, is related with the reduction of the computational cost, based on the use of the splitting technique to discretize in time, which means that at each time level the value of the numerical solution of all components can be decoupled. To confirm this fact, we solve example (56) with a classical algorithm which combines the implicit Euler method to discretize in time, on a uniform mesh, and the upwind scheme on the same Shishkin mesh as before to discretize in space. Note that this method does not decouple the components of the numerical solution. Table 3 shows the ratio between the maximum errors obtained using our method and the ones related to the classical method, for the same values of the diffusion parameter ε ; for each value of ε_3 the first row corresponds to the ratios for the first component, the second row for the second component and the last row for the third component. From this table, it is clear that the maximum errors obtained with our algorithm are similar to the obtained ones with the classical first order method.

Next, we compare the computational cost of the classical method and our algorithm. We solve examples (53) and (56) for some values of N , $M = N/2$ and fixed values of the diffusion parameters. Tables 4 and 5 show the required CPU time in seconds using the splitting and the classical algorithms respectively. All results are obtained in a PC with an i5 processor, 1.80 GHz, using Fortran Gnu. We can observe that the CPU time tends to enlarge 4 times in both methods as long as N doubles, as it was expected. Notice that, from the n^2 factor of decreasing in terms of computational complexity of our algorithm, respect to the classical method used to compare it, a speed up is produced in our method when the number of

Table 3
Ratio between the maximum errors of our method and the classical one for example (56).

ε_3	$N = 32$	$N = 64$	$N = 128$	$N = 256$	$N = 512$
2^{-6}	1.016	1.009	1.009	1.005	1.005
	0.988	0.993	0.994	0.995	0.995
	0.996	0.997	0.998	0.998	1.031
2^{-8}	0.994	1.009	1.009	1.005	1.005
	0.986	0.992	0.993	0.994	0.995
	0.996	0.998	0.998	0.998	1.017
2^{-10}	1.017	1.009	1.009	1.005	1.005
	0.985	0.992	0.993	0.994	0.995
	0.996	0.997	0.998	0.998	1.017
...
2^{-24}	1.017	1.009	1.009	1.005	1.005
	0.985	0.991	0.993	0.994	0.995
	0.996	0.998	0.998	0.998	0.998

Table 4
CPU time for example (53) for $\varepsilon_2 = 2^{-16}$ and $\varepsilon_1 = 2^{-20}$.

	$N = 192$	$N = 384$	$N = 768$	$N = 1536$	$N = 3072$
classical	0.06250	0.28125	1.09375	4.39063	17.60938
splitting	0.06250	0.26563	1.03125	4.06250	16.32813
ratio	1	1.059	1.061	1.081	1.078

Table 5
CPU time for example (56) for $\varepsilon_3 = 2^{-12}$, $\varepsilon_2 = 2^{-16}$ and $\varepsilon_1 = 2^{-20}$.

	$N = 192$	$N = 384$	$N = 768$	$N = 1536$	$N = 3072$
classical	0.12500	0.56251	2.29688	8.98438	36.03125
splitting	0.06250	0.26563	1.12500	4.51563	18.09375
ratio	2	2.118	2.042	1.990	1.991

components n in the system (1) increases; Tables 4 and 5 show the CPU times associated to our method and the classical one and also the ratio between them, for examples (53) and (56) respectively; from these tables, we observe that in example (53) the CPU times are similar, whereas for example (56) the CPU time related to the classical method is around twice the related one to our method. These ratios increase strongly when the number of components in the system increase.

6. Conclusions

We have developed a robust and efficient numerical algorithm for solving a class of parabolic one-dimensional singularly perturbed systems of convection-diffusion type, where the convection matrix is diagonal and the diffusion parameters at each equation can be different, permitting that they have different orders of magnitude. The proposed method combines the fractional implicit Euler method together a splitting by components, to discretize in time, and the upwind scheme, to discretize in space, defined on a special nonuniform mesh of Shishkin type. The fully discrete scheme calculates the numerical solution by solving only tridiagonal linear systems; then, from the point of view of the computational cost, the method is better than other classical implicit methods which require to solve banded linear systems. We have shown that the efficiency of the algorithm increases when the number of components in the system grows. Some numerical results for two test problems are displayed, which corroborate in practice the good properties of the algorithm, according to the theoretical results.

Acknowledgements

The authors thank the referees for their valuable suggestions which have helped to improve the presentation of this paper. This research was partially supported by the project MTM2017-83490-P, the Aragon Government and European Social Fund (group E24-17R) and the Public University of Navarre, project PRO-UPNA 6158.

References

- [1] S. Bellew, E. O’Riordan, A parameter robust numerical method for a system of two singularly convection-diffusion equations, *Appl. Numer. Math.* 51 (2004) 171–186.
- [2] Z. Cen, Parameter-uniform finite difference scheme for a system of coupled singularly perturbed convection-diffusion equations, *J. Syst. Sci. Complex.* 18 (4) (2005) 498–510.
- [3] C. Clavero, J.L. Gracia, Uniformly convergent additive finite difference schemes for singularly perturbed parabolic reaction-diffusion systems, *Comput. Math. Appl.* 67 (2014) 655–670.
- [4] C. Clavero, J.L. Gracia, Uniformly convergent additive schemes for 2D singularly perturbed parabolic systems of reaction-diffusion type, *Numer. Algorithms* 80 (2019) 1097–1120.
- [5] C. Clavero, J.C. Jorge, Uniform convergence and order reduction of the fractional implicit Euler method to solve singularly perturbed 2D reaction-diffusion problems, *Appl. Math. Comput.* 287 (88) (2016) 12–27.
- [6] C. Clavero, J.C. Jorge, Solving efficiently one dimensional parabolic singularly perturbed reaction-diffusion systems: a splitting by components, *J. Comput. Appl. Math.* 344 (2018) 1–14.
- [7] C. Clavero, J.C. Jorge, An efficient numerical method for singularly perturbed time dependent parabolic 2D convection-diffusion systems, *J. Comput. Appl. Math.* 354 (2019) 431–444.
- [8] P.A. Farrell, A.F. Hegarty, J.J.H. Miller, E. O’Riordan, G.I. Shishkin, *Robust Computational Techniques for Boundary Layers*, Applied Mathematics, vol. 16, Chapman and Hall/CRC, 2000.
- [9] J.L. Gracia, F. Lisbona, A uniformly convergent scheme for a system of reaction–diffusion equations, *J. Comput. Appl. Math.* 206 (2007) 1–16.
- [10] S.S. Kalaiselvan, J.J.H. Miller, S. Valarmathi, A parameter uniform fitted mesh method for a weakly coupled system of two singularly perturbed convection-diffusion equations, *Math. Commun.* 24 (2019) 193–210.
- [11] R.R. Kellogg, N. Madden, M. Stynes, A parameter-robust numerical method for a system of reaction-diffusion equations in two dimensions, *Numer. Methods Partial Differ. Equ.* 24 (1) (2008) 312–334.
- [12] M. Kumar, S. Natesan, Numerical analysis of singularly perturbed system of parabolic convection-diffusion problem with regular boundary layers, *Differ. Equ. Dyn. Syst.* (2019), <https://doi.org/10.1007/s12591-019-00462-2>.
- [13] M. Kumar, S. Natesan, A robust computational method for singularly perturbed system of 2D parabolic convection-diffusion problems, *Int. J. Math. Model. Numer. Optim.* 9 (2) (2019) 127–157.
- [14] M. Kumar, S. Natesan, Numerical simulation and convergence analysis for singularly perturbed system of parabolic convection-diffusion problems with interior layers, preprint.
- [15] R.B. Kellogg, A. Tsan, Analysis of some difference approximations for a singular perturbation problem without turning points, *Math. Comput.* 32 (44) (1978) 1025–1039.
- [16] O.A. Ladyzhenskaya, V.A. Solonnikov, N.N. Uraltseva, *Linear and Quasilinear Equations of Parabolic Type*, Translations of Mathematical Monographs, vol. 23, American Mathematical Society, Providence, RI, 1967.
- [17] T. Linss, Analysis of an upwind finite-difference scheme for a system of coupled singularly perturbed convection-diffusion equations, *Computing* 79 (2007) 23–32.
- [18] T. Linss, M. Stynes, Numerical solution of systems of singularly perturbed differential equations, *Comput. Methods Appl. Math.* 9 (2009) 165–191.
- [19] L.B. Liu, Y. Chen, A robust adaptive grid method for a system of two singularly perturbed convection-diffusion equations with weak coupling, *J. Sci. Comput.* 61 (2014) 1–16.
- [20] L.B. Liu, G. Long, Y. Zhang, Parameter uniform numerical method for a system of two coupled singularly perturbed parabolic convection-diffusion equations, *Adv. Differ. Equ.* 2018 (2018) 450, <https://doi.org/10.1186/s13662--018--1907--1>.
- [21] N. Madden, M. Stynes, A uniformly convergent numerical method for a coupled system of two singularly perturbed linear reaction-diffusion problems, *IMA J. Numer. Anal.* 23 (2003) 627–644.
- [22] J.J.H. Miller, E. O’Riordan, G.I. Shishkin, *Fitted Numerical Methods for Singular Perturbation Problems*, revised edition, World Scientific, 2012.
- [23] C.V. Pao, *Nonlinear Parabolic and Elliptic Equations*, Plenum Press, New York, 1992.
- [24] R.M. Priyadharshini, N. Ramanujam, A. Tamilsivan, Hybrid difference schemes for a system of singularly perturbed convection-diffusion equations, *J. Appl. Math. Inform.* 27 (2009) 1001–1015.
- [25] H.G. Roos, C. Reibiger, Analysis of a strongly coupled system of two convection-diffusion equations with full layer interaction, *Z. Angew. Math. Mech.* 91 (2011) 537–543.
- [26] H.G. Roos, M. Stynes, L. Tobiska, *Robust Numerical Methods for Singularly Perturbed Differential Equations*, Springer Series in Computational Mathematics, 2008, Berlin.
- [27] M. Stephens, N. Madden, A parameter-uniform Schwarz method for a coupled system of reaction–diffusion equations, *J. Comput. Appl. Math.* 230 (2009) 360–370.